Accelerated Publications

Liposome-Catalyzed Unfolding of Acetylcholinesterase from *Bungarus fasciatus*†

Irina Shin,‡ Israel Silman,‡ Cassian Bon,§ and Lev Weiner*,‖

Department of Neurobiology and Chemical Services, Weizmann Institute of Science, Rehovot 76100, Israel, and Unité des Venins, Institut Pasteur, 75724 Paris, France

Received December 8, 1997; Revised Manuscript Received February 10, 1998

ABSTRACT: The kinetics of thermal inactivation of acetylcholinesterase from the venom of the snake, *Bungarus fasciatus*, were studied at 45−54 °C. An Arrhenius plot reveals an activation energy of 113 kcal/mol. The thermally denatured enzyme displays the spectroscopic characteristics of a partially unfolded 'molten globule' state. The rate of thermal denaturation is greatly enhanced in the presence of unilamellar vesicles of dimyristoylphosphatidylcholine, the energy barrier for the transition being lowered from 113 to 52 kcal/mol. In contrast to our findings for partially unfolded *Torpedo californica* acetylcholinesterase [Shin et al. (1997) *Proc. Natl. Acad. Sci. U.S.A. 94*, 2848−2852], the thermally denatured snake enzyme does not remain bound to the liposomes but is released after unfolding and subsequently aggregates. The liposomes thus serve as catalysts for unfolding of the snake enzyme, and its rate of unfolding in the presence of liposomes can be described by the Michaelis−Menten equation ($K_m = 8 \times 10^{-7}$ M). The phospholipid vesicles display a catalytic turnover number of $k_{cat} \sim 4$ min^{-1}, assuming 15 binding sites per vesicle for the snake acetylcholinesterase.

The kinetics and thermodynamics of interaction of proteins with the lipid bilayer are a requirement for understanding their mode(s) of insertion into and translocation across biological membranes (*1*, *2*). These, in turn, are important for understanding both cotranslational and posttranslational cellular traffic of proteins (*3*−*5*). Endo et al. (*6*) showed that binding of a tightly folded precursor protein to the mitochondrial outer membrane involves a lipid-mediated conformational change, and a globular fragment of the bacterial toxin (colicin) undergoes a liposome-induced unfolding concomitantly with insertion into the lipid bilayer (*7*, *8*). We showed recently that unilamellar liposomes composed of dimyristoylphosphatidylcholine (DMPC)[1] greatly enhance the rate of unfolding of a dimeric form of *Torpedo californica* acetylcholinesterase (*Tc*AChE) to a partially unfolded state displaying the physicochemical features of a molten globule (MG) species (*2*). Unfolding of the native (N) water-soluble species occurred with concomitant incorporation of the MG into the lipid bilayer. Arrhenius plots revealed that the enhanced rate of unfolding was due to a dramatic lowering of the activation energy for the N⇒MG transition from 145 to 47 kcal/mol. Our data suggested that either the native enzyme or a quasi-native state with which it is in equilibrium interacts with the liposome, which then promotes a fast transition to the membrane-bound MG state by lowering the energy barrier for the transition. These findings raise the possibility that the membrane itself, by lowering the energy barrier for the N⇒MG transition, may play an active posttranslational role in insertion and translocation of proteins in situ.

In the following, we show that DMPC liposomes, by lowering the activation energy, similarly enhance the rate of thermal denaturation of a monomeric form of AChE purified from the venom of the Chinese krait, *Bungarus fasciatus* (*Bf*AChE; *9*, *10*). In this case, however, the MG species generated does not remain bound to the liposome, which thus serves as a catalyst of the unfolding process.

MATERIALS AND METHODS

Materials. *Bf*AChE was purified from *B. fasciatus* venom by affinity chromatography (*9*). Tris hydrochloride, acetylthiocholine, 5,5′-dithiobis(2-nitrobenzoic acid), 1-anilino-8-naphthalenesulfonic acid (ANS), and lysophosphatidylcholine (LysoPC) were from Sigma (St. Louis, MO). Sodium cholate was from Serva (Heidelberg, Germany). Synthetic DMPC and dansyl phosphatidylethanolamine (DsPE) were from Avanti Polar Lipids, Inc. (Alabaster, AL). Guanidine hydrochloride (Gdn-HCl) (ultrapure) was from Schwartz/Mann (Cleveland, OH). All other reagents were of analytical grade or higher.

† I. Silman is the Bernstein-Mason Professor of Neurochemistry, and I. Shin is supported by the Gilady Program for Immigrant Scientists of the Israeli Ministry of Absorption.

* To whom correspondence should be addressed. Fax: 972-8-9344142.

‡ Department of Neurobiology.

§ Unité des Venins.

‖ Chemical Services.

[1] Abbreviations: DMPC, dimyristoylphosphatidylcholine; *Tc*AChE, *Torpedo californica* acetylcholinesterase; MG, molten globule; N, native; *Bf*AChE, *Bungarus fasciatus* acetylcholinesterase; ANS, 1-anilino-8-naphthalenesulfonic acid; LysoPC, lysophosphatidylcholine; DsPE, dansyl phosphatidylethanolamine; Gdn-HCl, guanidine hydrochloride; CD, circular dichroism; U, unfolded; CMC, critical micelle concentration.

S0006-2960(97)03005-5 CCC: $15.00
Published on Web 03/10/1998

Buffers. Unless otherwise stated, the buffer employed was 0.1 M NaCl/10 mM Tris, pH 8.0 (buffer 1).

Assay Methods. *Bf*AChE concentrations were determined as described (*11*) or by measuring intrinsic fluorescence, exciting at 280 nm, and measuring emission at 340 nm. AChE activity was monitored as previously (*11*).

Liposomes. Small unilamellar phospholipid vesicles were prepared as described (*12*). Dansyl-labeled liposomes were prepared similarly, using a ratio of DMPC to DsPE of 100:1. Electron microscopy, using negative staining with uranyl acetate, revealed a population of unilamellar vesicles of diameter 300−500 Å (*12*), in the range to be expected for unilamellar vesicles (*13*). The number of vesicles was estimated on the assumption that one lipid molecule occupies ~0.7 nm^2 of vesicle surface area (*14*), assuming an average vesicle diameter of 400 Å. From these two numbers, one can calculate that each vesicle contains, on the average, ~7200 phospholipid molecules with molecular weight ~4.9 × 10^6. Large unilamellar vesicles were prepared as described (*15*).

Sucrose Gradient Centrifugation. Analytical sucrose gradient centrifugation was performed on 5−20% sucrose gradients made up in buffer 1 (*16*).

Interaction of *Bf*AChE with DMPC liposomes was investigated by a flotation-gradient centrifugation technique (*17*). A 30 μL sample of *Bf*AChE (1.2 mg/mL) was inactivated in the presence of 270 μL of DMPC liposomes (4 mg/mL) at 48 °C. When *Bf*AChE activity was <0.5%, the reaction mixture was loaded onto the sucrose step gradient, centrifuged, and analyzed as described previously (*12*).

Fluorescence Measurements. Intrinsic fluorescence of *Bf*AChE and ANS binding were measured in a Shimadzu RF-540 spectrofluorometer essentially as described earlier (*16*).

Titration of Dansyl-Labeled DMPC Liposomes with BfAChE. Fluorescence of dansyl-labeled DMPC liposomes was measured in a PTI Deltascan 400 spectrofluorometer at 28 °C. A 4 mm × 4 mm cuvette was employed, with magnetic stirring to maintain a homogeneous suspension. Temperature control was with a circulating water bath. Excitation was at 340 nm, and emission was measured at 390−650 nm. Dansyl-labeled DMPC liposomes (0.1 mg/mL) were titrated with *Bf*AChE (6.3 mg/mL), and the titration was monitored at 470 nm, at which wavelength the effect of the protein on dansyl fluorescence was maximal.

CD Measurements. Circular dichroism (CD) spectra were recorded in a Jasco J-500C spectropolarimeter as described previously (*16*). Data are expressed as the mean residue ellipticity, [Θ] (deg cm^2 $dmol^{-1}$).

RESULTS

Thermal Denaturation of BfAChE. To examine the effect of liposomes on the thermal denaturation of *Bf*AChE, we first studied the kinetics of deactivation and denaturation of native *Bf*AChE in the absence of liposomes as well as the spectral characteristics of the product of thermal denaturation.

No spontaneous inactivation of *Bf*AChE is observed at room temperature, but significant irreversible thermal denaturation can be monitored at 45 °C at pH 8.0 (Figure 1), with half-life ~90 min. It was shown earlier that thermal denaturation of *Tc*AChE obeys first-order kinetics (*16*), and

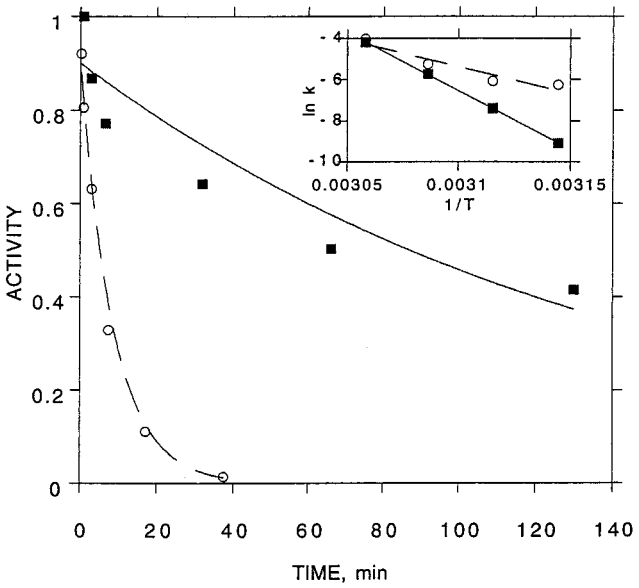

FIGURE 1: Effect of liposomes on thermal inactivation of *Bf*AChE. Samples of *Bf*AChE (0.5 μM) were incubated at 45 °C. Aliquots were withdrawn at appropriate times for assay of enzymic activity. (■) control; (○), in the presence of DMPC liposomes (5 mg/mL). Inset: Arrhenius plots of the temperature dependence of the rate of thermal inactivation of native AChE in the presence (○) and absence (■) of DMPC liposomes.

the same holds true for *Bf*AChE. First-order rate constants so obtained, in the range of 45−54 °C, permitted construction of an Arrhenius plot from which an activation energy of 113 kcal/mol could be calculated (Figure 1, inset). This is in good agreement with the value of 103 kcal/mol obtained by differential scanning calorimetry (Shnyrov, Silman, Bon, and Weiner, to be published).

Both mild thermal denaturation and exposure to low concentrations of Gdn-HCl (1.2−1.5 M) convert native *Tc*AChE to a partially unfolded state with the physicochemical characteristics of an MG (*16*, *18*, *19*). To characterize thermally denatured *Bf*AChE, we applied CD spectroscopy, intrinsic protein fluorescence, and fluorescence of the amphiphilic probe, ANS (Figure 2). For comparison, the spectral characteristics of *Bf*AChE in 1.5 and 5.0 M Gdn-HCl are shown. *Bf*AChE equilibrated in 5.0 M Gdn-HCl displays a broad emission spectrum with a maximum at 354 nm, typical of an unfolded (U) state (*20*). Furthermore, ellipticity in the far UV is greatly decreased, the CD band in the near UV is collapsed, and no binding of ANS is observed (Figure 2C). Both thermally denatured *Bf*AChE and *Bf*AChE in 1.5 M Gdn-HCl appear to be partially unfolded, since the intrinsic fluorescence emission maximum is at 341 nm and intermediate between that of native enzyme, N (336 nm), and of U (354 nm). The CD spectrum in the near UV indicates that the tertiary structures of both the thermally denatured enzyme and that in 1.5 M Gdn-HCl are largely destroyed. Both are also characterized by reduced ellipticity at 222 nm and by a concomitant reduction in both α-helical and β-sheet content, calculated according to Greenfield and Fasman (*21*) and Batra et al. (*22*), as compared to native *Bf*AChE (Table 1). The ellipticity in the far UV is, however, substantially greater than that of the enzyme in the fully unfolded (U) state in 5.0 M Gdn-HCl, as had been observed previously for *Tc*AChE (*18*). Also, as previously observed for *Tc*AChE, both thermally denatured *Bf*AChE and

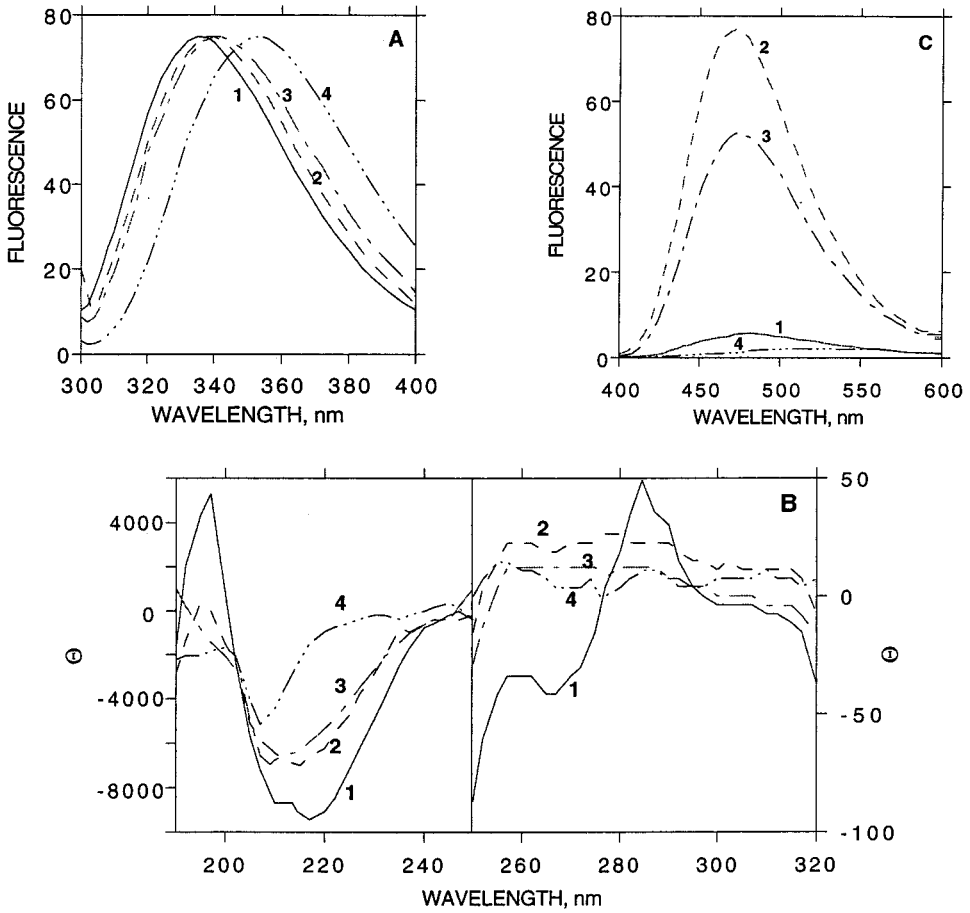

FIGURE 2: Spectral characteristics of thermally inactivated *Bf*AChE. Native *Bf*AChE was inactivated by heating at 53 °C for 5 min. (A) Normalized intrinsic fluorescence emission spectra (*Bf*AChE concentration, 2 μM). (B) CD spectra in the far and near UV (*Bf*AChE concentration, 8 μM). (C) ANS fluorescence emission spectra (*Bf*AChE concentration, 0.1 μM; ANS concentration, 0.1 mM). 1, Native *Bf*AChE; 2, thermally inactivated *Bf*AChE; 3, *Bf*AChE in 1.5 M Gdn-HCl; 4, *Bf*AChE in 5 M Gdn-HCl.

*Bf*AChE in 1.5 M Gdn-HCl produce a large increase in ANS fluorescence, characteristic of the MG state, and other partially unfolded conformations (*23*, *24*), whereas little or no increase in ANS fluorescence is observed in the presence of either N or U *Bf*AChE (Figure 2C).

Effect of Liposomes on Thermal Inactivation of BfAChE. Figure 1 compares the rates of thermal inactivation of *Bf*AChE in the presence and absence of unilamellar DMPC liposomes at pH 8 and 45 °C. In the presence of the liposomes, the half-life of inactivation was decreased from ~90 to ~6 min. Similar experiments were performed at 45−54 °C. The first-order rate constants thus obtained were used to construct Arrhenius plots which revealed that the activation energy for thermal denaturation is lowered from 113 to 52 kcal/mol in the presence of liposomes (Figure 1, inset).

Interaction of BfAChE with DMPC Liposomes. The acceleration of thermal inactivation of *Bf*AChE by DMPC liposomes demonstrates that the enzyme is interacting with the lipid bilayer. In the case of *Tc*AChE, we showed earlier that accelerated thermal inactivation in the presence of DMPC liposomes resulted in concomitant attachment of the partially unfolded enzyme to the liposomes (*2*). Interaction of thermally inactivated *Bf*AChE with the DMPC vesicles was investigated by a flotation-gradient centrifugation technique that permits separation of free and liposome-bound enzyme (*2*, *12*, *17*). In contrast to what was observed for *Tc*AChE, thermally denatured *Bf*AChE does not remain bound to the DMPC vesicles (Figure 3); whereas the liposomes float to the top of the gradient, the thermally inactivated *Bf*AChE remains at the bottom.

Table 1: Estimated Percentages of a α Helix, β Structure, and Random Coil of *Bf*AChE from CD Curves[a]

state	α helix (%)	β structure (%)	random coil (%)
native	23	37	40
heat-denatured	14	26	60
1.5 M Gdn-HCl	13	27	60
5 M Gdn-HCl	1	19	80

[a] The α-helical content, F_h, was calculated using the equation: $F_h = (-[Q^{222}] + 260)/35\,740$ according to Batra et al. (*22*). β-structure and random coil content were evaluated according to Greenfield and Fasman (*21*).

The fact that the unfolded *Bf*AChE does not remain bound to the liposomes suggests that, in effect, they are catalyzing the unfolding reaction. Thus the native protein may be considered as a substrate for the liposome and the partially unfolded protein as a product. In fact, liposome-accelerated inactivation of *Bf*AChE, as a function of the concentration, may be described by a Michaelis−Menten plot with *Bf*AChE as the substrate and the DMPC liposomes as the catalyst (Figure 4A), with the rate of inactivation approaching a saturation value above 6 μM. Plotting the data according to the Lineweaver−Burk equation yields a straight line (Figure 4B) from which an apparent K_m value of 8×10^{-7} M can be extracted for interaction of *Bf*AChE with the

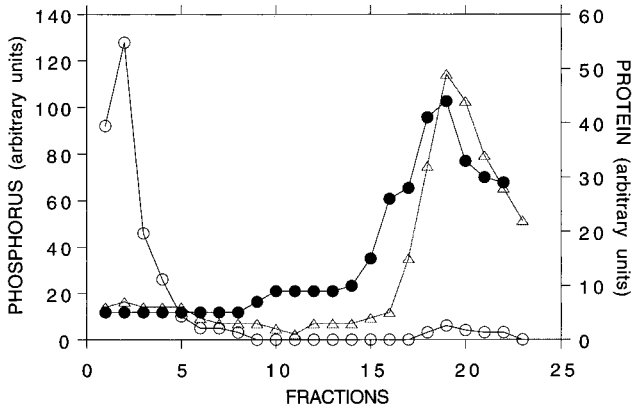

FIGURE 3: Flotation gradient centrifugation profiles of native and thermally inactivated *Bf*AChE in the presence of DMPC liposomes. Flotation gradients were constructed as described under Methods. Native *Bf*AChE (2−3 mg/mL) was incubated for 1 h at 25 °C with DMPC liposomes (10 mg/mL) before loading onto the gradients. 30 μL of *Bf*AChE (1.2 mg/mL) was inactivated in the presence of 270 μL DMPC liposomes (4 mg/mL) at 48 °C. When *Bf*AChE activity had decreased to <0.5% of control activity, the reaction mixture was loaded onto the flotation gradient. Liposomes floated to the top of gradient, i.e., to the left of the figure, as measured by monitoring phosphorus (○). (●) native *Bf*AChE; (△) *Bf*AChE after thermal inactivation in the presence of DMPC liposomes.

liposomes. We earlier showed that 7−8 molecules of the *Tc*AChE dimer were bound to the DMPC liposomes at saturation (*12*). If it is assumed that ca. 15 molecules of the monomeric *Bf*AChE per liposome are bound at saturation, a catalytic turnover number of $k_{cat} \sim 4$ min^{-1} can be calculated.

The rate of thermal inactivation of *Bf*AChE, at 45 °C, as a function of the liposome concentration was investigated. The rate of inactivation increases linearly with liposome concentration in the concentration range 0−1.5 μM (data not shown). This confirms our assumption that the liposomes are catalyzing the unfolding process.

Although sucrose gradient centrifugation (see above) revealed that the MG species produced by thermal denaturation does not remain tightly bound to the DMPC liposomes, this is not an equilibrium measurement. It might indeed be expected that the partially unfolded species, due to its exposed hydrophobic surfaces, would display higher affinity for the liposome than native *Bf*AChE. One might thus predict that addition of enzyme which had already been thermally inactivated would inhibit liposome-catalyzed inactivation of freshly added native *Bf*AChE by reducing the area on the liposome surface available for catalysis of its unfolding. Figure 5 shows that the presence of previously inactivated *Bf*AChE has no measurable effect on the rate of inactivation of a freshly added portion of native enzyme. This demonstrates that the partially unfolded enzyme does not associate strongly with the liposome surface under equilibrium conditions.

Titration of Fluorescently Labeled Liposomes by BfAChE. To quantitate the interaction of native *Bf*AChE with the DMPC liposomes, a dansyl conjugate of PE was employed as a fluorescent probe (*25*, *26*). Figure 6 shows the fluorescence emission spectra of DMPC vesicles containing 1% dansyl-PE in the absence and presence of native *Bf*AChE. Addition of *Bf*AChE resulted in an increase in dansyl fluorescence and in a blue shift in the emission maximum (Figure 6). If it is assumed that interaction between *Bf*AChE and the dansyl-labeled liposomes can be represented by the scheme:

$$E + L \rightleftharpoons EL$$

where E, L, and EL are enzyme, liposome, and enzyme−liposome complex, respectively, and it is further assumed that [E] > [L], the following equation can be derived:

$$1/(F - F_o) = 1/K_A F_B[L] + [E]/F_B\,[L]$$

where F is the experimentally measured fluorescence, and F_o and F_B are respectively the fluorescence in the absence of protein and the fluorescence at saturation, and K_A is the association constant. Figure 6 (inset) shows the plot obtained by using this equation, from which a value of $K_d = 1/K_a = 3 \times 10^{-6}$ M was obtained. It should be emphasized that titration of the dansyl-labeled DMPC vesicles by native *Bf*AChE was performed at 28 °C. At this temperature, the enzyme retained full catalytic activity over the time course of the experiment.

Aggregation in the Process of Thermal Denaturation of BfAChE. Thermal denaturation of proteins is often accompanied by aggregation, due mostly to exposure of hydrophobic surfaces in the partially unfolded protein (*27*).

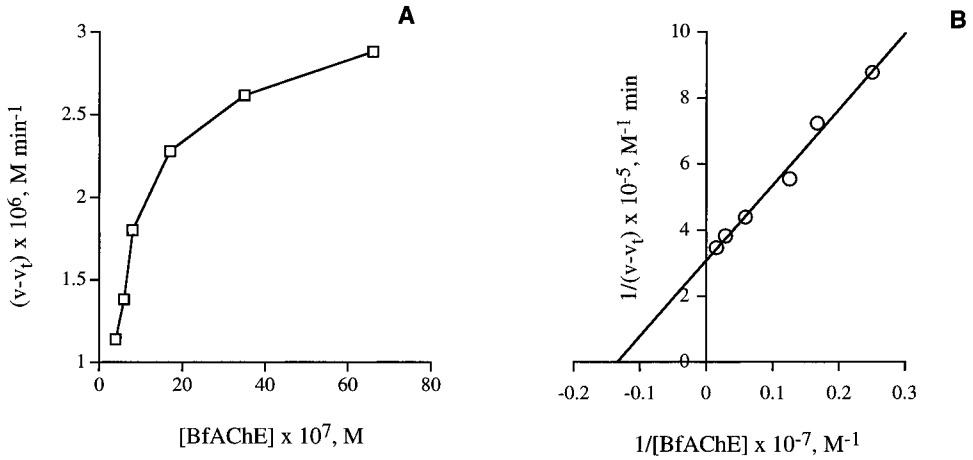

FIGURE 4: Kinetic analysis of catalysis of thermal inactivation of *Bf*AChE by DMPC liposomes. Inactivation was performed at 45 °C. (A) Michaelis−Menten plot; (B) Lineweaver−Burk plot. v and v_t are, respectively, the rates of thermal inactivation of *Bf*AChE in the presence and absence of liposomes.

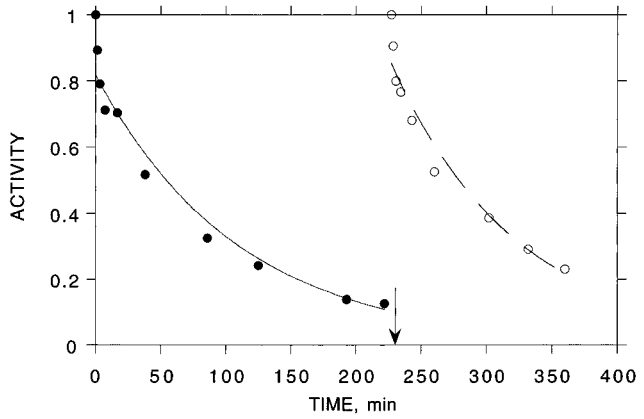

FIGURE 5: Effect of thermally inactivated *Bf*AChE on the rate of thermal denaturation of freshly added native *Bf*AChE in the presence of liposomes. *Bf*AChE (0.6 μM) was inactivated in the presence of DMPC liposomes (0.15 μM vesicle concentration) at 45 °C. After 4 h, when *Bf*AChE activity was ~10% of control activity, a fresh aliquot of native *Bf*AChE was added to a final concentration of 0.6 μM. The arrow marks the time of addition of the fresh aliquot.

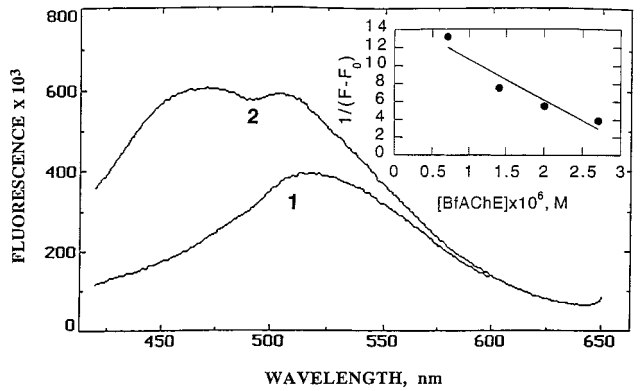

FIGURE 6: Fluorescence emission spectra of dansyl-labeled DMPC liposomes in the absence (1) and presence (2) of native *Bf*AChE (2.5 μM). The dansyl-labeled liposomes were prepared as described under Methods. The lipid concentration was 1 mg/mL. Inset: Titration of dansyl-labeled liposomes with *Bf*AChE, monitored at 470 nm. Measurements were performed at 28 °C.

Sucrose gradient centrifugation revealed that thermally denatured *Bf*AChE aggregates rapidly (Figure 7A). Thus, after 5 min at 53 °C, which results in >99% inactivation, <10% of the denatured enzyme can be found in a ca. 4.55 S peak, corresponding to the monomeric species (*9*, *28*). If thermal denaturation is carried out at in the presence of DMPC liposomes 51 °C, a temperature at which the rate of inactivation is similar to that at 53 °C in the absence of liposomes, a similar sucrose gradient profile is obtained (Figure 7B). Thus, the liposomes have no effect on the rate of aggregation of the thermally denatured *Bf*AChE.

Mechanism of the Interaction of BfAChE with Lipid Bilayer. We showed earlier that, under conditions in which native *Tc*AChE alone is stable and catalytically active for many hours, DMPC liposomes promote a rapid transition to the MG state in which the protein remains bound to the membrane (*2*). For *Bf*AChE, the liposomes also lower substantially the energy barrier for transition to the MG state, but the partially unfolded *Bf*AChE so generated does not remain bound to the membrane. To better understand the role of the membrane in the unfolding process, we compared the effect of large unilamellar DMPC vesicles (LUV),

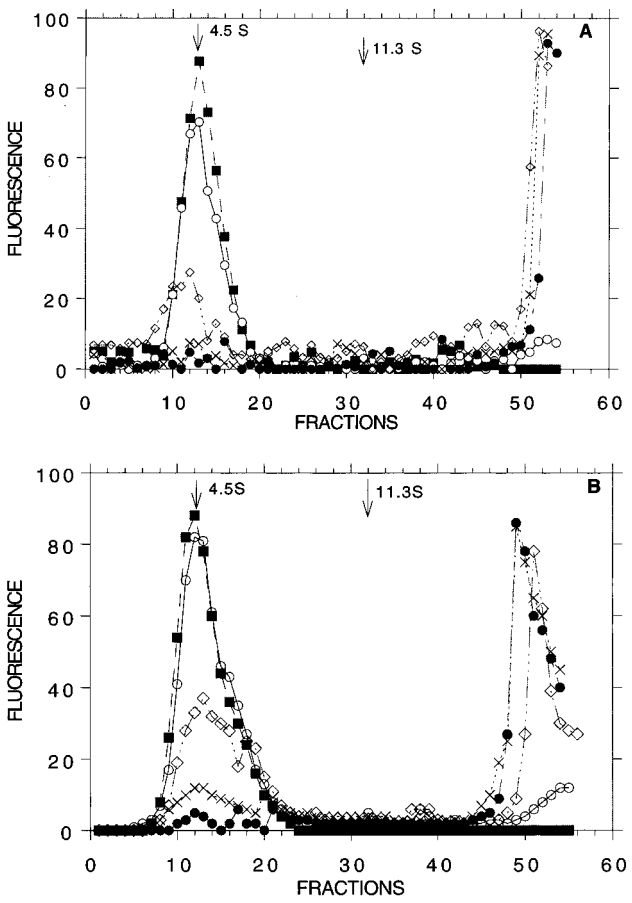

FIGURE 7: Sucrose gradient centrifugation profiles of native and thermally denatured *Bf*AChE in the absence and presence of DMPC liposomes. (■) Native *Bf*AChE; (○), *Bf*AChE denatured by heating for 1 min; (◊), *Bf*AChE denatured by heating for 3 min; (×), *Bf*AChE denatured by heating for 5 min; (●), *Bf*AChE denatured by heating for 15 min. Arrows mark the positions of catalase (11.3 S) and of the peak of enzymic activity of native *Bf*AChE (4.5 S), which served as markers. A) Thermal denaturation at 53 °C in the absence of liposomes. (B) Thermal denaturation at 51 °C in the presence of liposomes. The liposome concentration was 10 mg/mL, and that of *Bf*AChE was 10 μM.

prepared according to Hope et al. (*15*), with that of the small unilamellar vesicles (SUV) employed for most of the study. Inactivation of *Bf*AChE at 45 °C in the presence of LUV proceeds much faster (k = 0.0564 min^{-1}) than in their absence (k = 0.0068 min^{-1}), but more slowly than in the presence of SUV at the same lipid concentration (k = 0.1141 min^{-1}). We earlier showed that MG species derived from *Tc*AChE bound well to SUV, but only poorly to LUV of the same lipid (DMPC) (*12*). Thus, liposome curvature may contribute to binding and, thereby, also to the rate of thermal denaturation of *Bf*AChE.

Analysis of the kinetics of thermal inactivation of *Bf*AChE as a function of the concentrations of LysoPC (Figure 8) and cholate (not shown) reveals that the rate of the thermal denaturation is not significantly affected by either the lysolipid or by cholate at concentrations below their critical micelle concentrations (CMC). Above the CMC, however, the rate of thermal denaturation increases linearly with the concentration of either compound. It could thus be concluded that the surface rather than its chemical constituents is responsible for enhancement of the rate of unfolding.

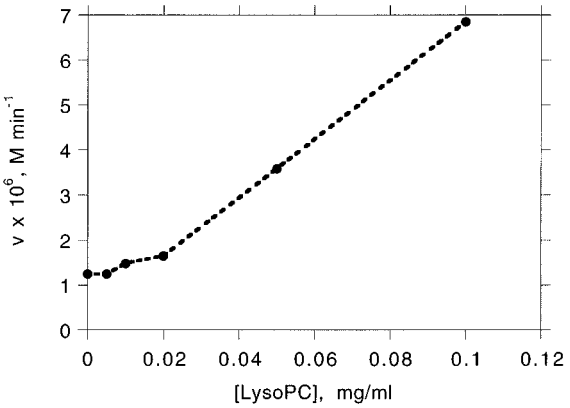

FIGURE 8: Concentration dependence of the effect of LysoPC on the rate of thermal denaturation of *Bf*AChE. Measurements were performed at 45 °C and a *Bf*AChE concentration of 0.5 μM. The CMC of LysoPC is 0.02 mg/mL.

DISCUSSION

We earlier demonstrated that the lipid bilayer could greatly accelerate inactivation of *Tc*AChE by lowering the energy barrier for transition from the native to a partially unfolded state with the characteristics of a MG species (*2*). The MG species so generated remained tightly bound to the liposome. The data presented above show that DMPC liposomes also increase the rate of the N⟹MG transition for *Bf*AChE. But the crucial difference, in the case of *Bf*AChE, is that the partially unfolded protein is released from membrane. Thus, the DMPC liposome serves as a catalyst of the N⟹MG transition. Indeed, we were able to show that the rate of transition can be described by Michaelis−Menten kinetics and to obtain an apparent K_m value at 45°, less than 4-fold lower than the dissociation constant for the complex of *Bf*AChE with the DMPC liposomes as determined directly by fluorescence quenching at 28°. It is important to note that when thermal denaturation of *Bf*AChE was performed in the presence of liposomes, sucrose gradient centrifugation revealed that a substantial monomer remained after thermal inactivation was essentially complete (Figure 7B). This permits the conclusion that the role of the liposomes is to accelerate inactivation rather than aggregation.

The effects of organic solvents on protein conformation has been investigated extensively (*29*−*31*). Methanol has been shown to induce transition of cytochrome *c* and β-lactoglobulin to MG-like states (*32*, *33*), and the authors believe that the polar solvent may be simulating conditions near the membrane surface where a low dielectric constant is believed to prevail. It was not, however, clear whether the transition could be ascribed to a change in the average dielectric constant of the solvent, to binding of the alcohol molecules to the polypeptide chain, or to an influence on water structure.

Our data clearly show that the surface itself as well as surface curvature play crucial roles in promoting the N⟹MG transition, since practically no effect of detergents was observed below the CMC (Figure 8) and small unilamellar DMPC vesicles were much more effective than the corresponding large unilamellar vesicles.

Our earlier study (*2*) showed that the lipid bilayer promoted an N⟹MG transition of *Tc*AChE with concomitant binding of the partially unfolded protein to the lipid bilayer. This is in contrast to the situation observed for *Bf*AChE, in which the partially unfolded protein is released from the membrane. It was shown that the peptide responsible for interaction of the MG species of *Tc*AChE with the bilayer membrane contains the most extended hydrophobic sequence in the protein, 35 amino acids (*12*). Three shorter hydrophobic peptides, which we identified on the basis of hydropathy plots, containing 22, 22, and 27 amino acids, did not appear to be involved in the enzyme−bilayer interaction. Inspection of the sequence of *Bf*AChE (*10*) using the same procedure employed for *Tc*AChE (*34*, *35*) reveals five hydrophobic stretches in *Bf*AChE. None of these sequences, which contain 16, 24, 19, 20, and 18 amino acids, respectively, is as long as the extended sequence in *Tc*AChE that was found to adhere to the liposome. Thus, none of them may possess the capacity to anchor the partially unfolded form of *Bf*AChE to the liposome surface. It should also be noted that *Tc*AChE is dimeric and thus can contribute two hydrophobic sequences to its anchoring, whereas *Bf*AChE is monomeric.

Whether movement occurs cotranslationally or posttranslationally, it is commonly accepted that proteins do not cross biological membranes in their native conformation (*3*). Furthermore, it is well documented that proteins in partially unfolded states can be trapped by molecular chaperones both in vitro and in vivo (*36*) and that chaperones play an important role in translocation of proteins across biological membranes (*4*). The fact that a lipid bilayer can actually catalyze the unfolding of a fully processed protein under physiological conditions suggests, in turn, that the plasma membrane may similarly act to generate partially unfolded species in vivo that can then serve as substrates for translocation, assembly, or degradation.

In recent years, evidence has accumulated that protein misfolding, resulting in misassembly of normally soluble proteins into fibrillar structures, may be a causative agent in a variety of amyloid and prion diseases (*37*). In some of these diseases, which may be referred to as 'conformational diseases' (*38*), at least part of the protein is correctly folded and released in its native form, and the disease condition arises from subsequent changes that lead to aggregation and deposition of the protein. It was recently shown that a MG state of a mutant lysozyme is the intermediate that leads to amyloid fibril formation in autosomal dominant hereditary amyloidosis resulting in familial visceral amyloidosis (*39*). It was earlier suggested that the scrapie prion protein has the conformational characteristics of an aggregated MG folding intermediate (*40*). The mechanism(s) of fibril formation are under active discussion (see, for example, refs *41* and *42*). Our finding that a lipid bilayer can catalyze partial unfolding of a native protein, with subsequent aggregation raises the possibility that the membranous structures within the cell may play a role in such conformational diseases.

ACKNOWLEDGMENT

We thank Bernard Saliou for his technical assistance in the purification of enzyme and Dmitry Gakamsky for his assistance in the fluorescence experiments of dansyl-labeled liposomes.

REFERENCES

1. Watts, A. (1995) *Biochem. Soc. Trans. 23*, 959−965.
2. Shin, I., Kreimer, D., Silman, I., and Weiner, L. (1997) *Proc. Natl. Acad. Sci. U.S.A. 94*, 2848−2852.
3. Rapoport, T., Jungnickel, B., and Kutay, U. (1996) *Annu. Rev. Biochem. 65*, 271−303.
4. Schatz, G., and Dobberstein, B. (1996) *Science 271*, 1519−1526.
5. Rothman, J. E., and Wieland, F. T. (1996) *Science 272*, 227−234.
6. Endo, T., Eilers, M., and Schatz, G. (1989) *J. Biol. Chem. 264*, 2951−2956.
7. van der Goot, F. G., Lakey, J. H., and Pattus, F. (1991) *Trends Cell Biol. 2*, 343−348.
8. Shin, Y.-K., Levinthal, C., Levinthal, F., and Hubbell, W. L. (1993) *Science 259*, 960−963.
9. Cousin, X., Créminon, C., Grassi, J., Méflah, K., Cornu, G., Saliou, B., Bon, S., Massoulié, J., and Bon, C. (1996) *FEBS Lett. 387*, 196−200.
10. Cousin, X., Bon, S., Duval, N., Massoulié, J., and Bon, C. (1996) *J. Biol. Chem. 271*, 15099−15108.
11. Dolginova, E., Roth, E., Silman, I., and Weiner, L. M. (1992) *Biochemistry 31*, 12248−12254.
12. Shin, I., Silman, I., and Weiner, L. M. (1996) *Protein Sci. 5*, 42−51.
13. Papahadjopoulos, D., and Miller, N. (1967) *Biochim. Biophys. Acta 135*, 624−638.
14. Small, D. M. (1986) in *Handbook of Lipid Research: The Physical Chemistry of Lipids: From Alkanes to Phospholipids* (Hanahan, D. J., Ed.) pp 43−88, Plenum Press, New York.
15. Hope, M. J., Bally, M. B., Webb, G., and Cullis, P. R. (1985) *Biochim. Biophys. Acta 812*, 55−65.
16. Kreimer, D. I., Shnyrov, V. L., Villar, E., Silman, I., and Weiner, L. (1995) *Protein Sci. 4*, 2349−2357.
17. Futerman, A. H., Fiorini, R. M., Roth, E., Low, M. G., and Silman, I. (1985) *Biochem. J. 226*, 369−377.
18. Kreimer, D. I., Szosenfogel, R., Goldfarb, D., Silman, I., and Weiner, L. (1994) *Proc. Natl. Acad. Sci. U.S.A. 91*, 12145−12149.
19. Kreimer, D. I., Shin, I., Shnyrov, A. L., Villar, E., Silman, I., and Weiner, L. (1996) *Protein Sci. 5*, 1852−1864.
20. Burstein, E. A., Vedenkina, N. S., and Ivkova, M. N. (1973) *Photochem. Photobiol. 18*, 263−279.
21. Greenfield, N., and Fasman, G. D. (1969) *Biochemistry 8*, 4108−4116.
22. Batra, P. P., Roebuck, M. A., and Uetrecht, D. (1990) *J. Protein Chem. 9*, 37−44.
23. Goto, Y., and Fink, A. L. (1989) *Biochemistry 28*, 945−952.
24. Ptitsyn, O. B. (1995) *Adv. Protein Chem. 47*, 83−229.
25. Bazzi, M. D., and Nelsestuen, G. L. (1987) *Biochemistry 26*, 115−122.
26. Junker, M., and Creutz, C. E. (1994) *Biochemistry 33*, 8930−8940.
27. Zale, S. E., and Klibanov, A. M. (1986) *Biochemistry 25*, 5432−5444.
28. Porschke, D., Créminon, C., Cousin, X., Bon, C., Sussman, J., and Silman, I. (1996) *Biophys. J. 70*, 1603−1608.
29. Singer, S. J. (1962) *Adv. Protein Chem. 17*, 1−68.
30. Timasheff, S. N. (1970) *Acc. Chem. Res. 3*, 62−68.
31. Schellman, J. A. (1987) *Biopolymers 26*, 549−559.
32. Bychkova, V. E., Dujsekina, A. E., Klenin, S. I., Tiktopulo, E. I., Uversky V. N., and Ptitsyn, O. B. (1996) *Biochemistry 35*, 6058−6063.
33. Uversky, V. N., Narizhneva, N. V., Kirschstein, S. O., Winter, S., and Lober, G. (1997) *Folding Des. 2*, 163−172.
34. Kyte, J., and Doolittle, R. F. (1982) *J. Mol. Biol. 157*, 105−132.
35. Eisenberg, D., Schwarz, E., Komaromy, M., and Wall, R. (1984) *J. Mol. Biol. 179*, 125−142.
36. Hartl, F. U. (1996) *Nature 381*, 571−579.
37. Kelly, J. W. (1997) *Structure 5*, 595−600.
38. Carrell, R. W., and Lomas, D. A. (1997) *Lancet 350*, 134−138.
39. Booth, D. R., Sunde, M., Bellotti, V., Robinson, C. V., Hutchinson, W. L., Fraser, P. E., Hawkins, P. N., Dobson, C. M., Radford, S. E., Blake, C. C. F., and Pepys, M. B. (1997) *Nature 385*, 787−793.
40. Safar, J., Roller, P. P., Gajdusek, D. C., and Gibbs, C. J., Jr. (1994) *Biochemistry 33*, 8375−8383.
41. Cohen, F. E., Pan, K.-M., Huang, Z., Baldwin, M. A., Fletterick, R. J., and Prusiner, S. B. (1994) *Science 264*, 530−531.
42. Lansbury, P. T., and Caughey, B. (1995) *Chem. Biol. 2*, 1−5.

BI973005Q